Jurnal Polimesin
Department of Mechanical Engineering
State Polytechnic of Lhokseumawe
http://e-jurnal.pnl.ac.id/polimesin
e-ISSN : 2549-1999 No. : 4 Month : August
p-ISSN : 1693-5462 Volume : 22 Year : 2024

Article Processing Dates: Received on 2024-04-18, Reviewed on 2024-05-20, Revised on 2024-07-12, Accepted on 2024-07-15 and Available online on 2024-08-30

The influence of Al-Ti-B on the microstructure of unidirectionally solidified Al-10wt.%Cu-10wt.%Si

Dedy Masnur[1*], Viktor Malau[2], Suyitno[3]
[1]Mechanical Engineering Department, Universitas Riau, Pekanbaru, 28293, Indonesia
[2]Mechanical Engineering Department, Universitas Gadjah Mada, Yogyakarta, 55281, Indonesia
[3]Mechanical Engineering Department, Universitas Tidar, Magelang, 56116, Indonesia
*Corresponding author: dedy.masnur@lecturer.unri.ac.id

Abstract

Many works have reported the role of grain refiners in aluminum-silicon alloy casting in direct chill casting. However, only a few are under the unidirectional solidification condition. Direct chill casting favors equiaxed structures, while unidirectional solidification favors columnar structures. This work investigated the influence of Al-Ti-B on the microstructure of unidirectionally solidified Al-10wt.%Cu-10wt.%Si. The samples were directionally solidified using the Bridgman apparatus. It was cooled at the bottom to a temperature of 650°C, and the temperatures were recorded during the cooling. A representation of the cooling curve was selected, and the solidification parameters were calculated. Metallographic procedures were applied to observe the microstructure across the sample length. The results show that the 0.03wt.%Ti effectively promotes nucleation in many sites. It leads to the formation of equiaxed structures and prevents fine columnar structures from further growth. Due to the magnitude of the cooling rate, the 0.03wt.%Ti exhibits fine columnar, fine equiaxed, coarse equiaxed, and dendrite equiaxed structures at the separated distance from the contact area. This formation is in line with the one produced by the mechanism in direct chill casting. Understanding the grain refiner effect is crucial for optimizing manufacturing processes and achieving desired material properties. The Al-Ti-B addition is not recommended in the propeller manufacturing industry.

Keywords:
Al-Cu-Si, columnar, grain refiner, unidirectional solidification.

1 Introduction

Metal casting has been an economical way to manufacture complex components. Recently, the development of this technique has involved 3D printing technology [1]. The mechanical properties of cast products are influenced by process parameters, namely pouring temperature [2], die temperature, material composition, modifier, and grain refiner.

Aluminum-Silicon (Al-Si) alloys are one of the selected materials that have been widely used in metal casting. The mechanical properties of aluminum-silicon can be improved by modifying the silicon eutectic morphology, grain size, shape, and microstructure parameters (primary and secondary dendrite arm spacing) [3], [4], and [5]. A low percentage of elements were added to the Al-Si alloys, namely, strontium (Sr), sodium (Na), potassium (K), calcium (Ca), antimony (Sb), arsenic (As), selenium (Se), niobium (Nb), and titanium (Ti). These elements induce a modification in eutectic morphology (modifier) and reduce the grain size (grain refiner) [3], [4], [6], [7], [8], [9], [10]. This modified structure plays an essential role in determining the final properties of the alloy; therefore, scientists have made considerable efforts to understand them.

Adding Ti in the form of Al-Ti-B master alloy reduces the grain size of Al-Si alloys. The Ti concentration and the holding time influence this reduction. 0.06wt.%Ti is required to produce grain sizes of 1 mm and 0.5 mm in Al-7wt.%Si [11] and A356 alloys, respectively [12]. 0.19%wt.%Ti reduces the grain size of Al-7wt.%Si-3wt.%Cu-Mg from 3.5 mm to 0.5 mm [7]. The grain size remains constant for further Ti addition. The minimum grain size can only be achieved within a particular holding time; beyond that time, the grain refiner dissolves into the aluminum, and the grain size increases. The holding time range is less than 3 minutes for commercially pure aluminum [13], less than 10 minutes for Al-7wt.%Si-0.3wt.%Mg [14], and less than 30 minutes for A356.

The grain refinement process in direct casting is described by the mechanisms [13], [14], [15], and [16]: once the Al-5wt.%Ti-B melts, it releases $TiAl_3$ crystal into the aluminum and dissolves. Ti enriches the crystal surface and begins to solidify at a temperature above the melting temperature of aluminum (665°C). α-Al crystals then grow around the surface of $TiAl_3$. After further cooling, the dendrite growth begins and ends when the solidification process is complete. This mechanism occurs in many sites and involves higher thermal gradients and faster cooling rates. It leads to a uniform distribution of $TiAl_3$ and Ti-B particles, which are critical for nucleation. As a result, uniform, fine structures are obtained.

Other works conducted in unidirectional solidification reported that adding Al-2wt.%Nb-xB produced fine-equiaxed crystals less dependent on the thermal gradient. The addition of Al-2wt.%NbxB also leads to the refinement of eutectic and primary silicon particles [8]. In contrast, adding Al-5wt.%Ti-1wt.%B to Al-10wt.%Si formed columnar grain [17]. The unidirectional solidification process provides a controllable environment with a lower thermal gradient, and nucleation occurs at a particular site. In the case of the addition of Al-Ti-B, the dispersed $TiAl_3$ crystals are supposed to initiate nucleation at many sites: however, the formed microstructure clearly shows the opposite.

The work in unidirectional solidification, especially in Al-Ti-B, is still limited to the produced microstructure. However, the mechanism of the grain refinement is still unexplained. This work investigates the influence of Al-Ti-B on the microstructure of unidirectionally solidified Al-10wt.%Cu-10wt.%Si.

2 Materials and Methods

2.1 Materials

Al-10wt.%Cu-10wt.%Si with (0.03wt.%Ti) and without 0.03wt.%Ti (base alloy) samples were prepared by combining aluminum AA1050, Al-40%Cu, Al-33.6%wt.%Si (master alloy), and Al-6Ti-B in the weighing amount. The percentage of 0.03wt.%Ti refers to [12] as sufficient to decrease the grain size. AA1050 and Al-40wt.%Cu were melted in a ceramic electric furnace at 700°C and kept at this temperature for 5 minutes. Al-6Ti-B was added to the melt and then stirred using the aluminum rod for 30 seconds. The melt was poured into the 6 mm diameter and 60 mm height cylinder-shaped cavity in a medium carbon steel die (Fig. 1).

The casted cylinders were inserted in the 6 mm inside diameter, 10 mm outside diameter, and 60 mm height hollow clay mold (Fig. 2). Six holes were prepared for embedding thermocouples in the mold wall. The first hole was 5 mm from the contact area, and the next five holes had 10 mm of distance between them. The clay mold was attached to the stainless-steel holder, with a ceramic pipe on the upper part. Those parts maintained the mold position during the unidirectional

solidification process. Similar steps, excluding the addition of Al-6Ti-B, were repeated for the preparation of the Al-10wt.%Cu-10wt.%Si samples.

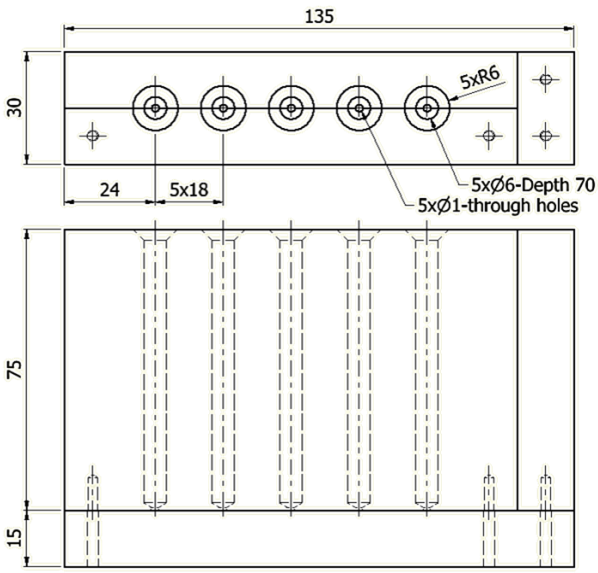

Fig. 1. Carbon steel die.

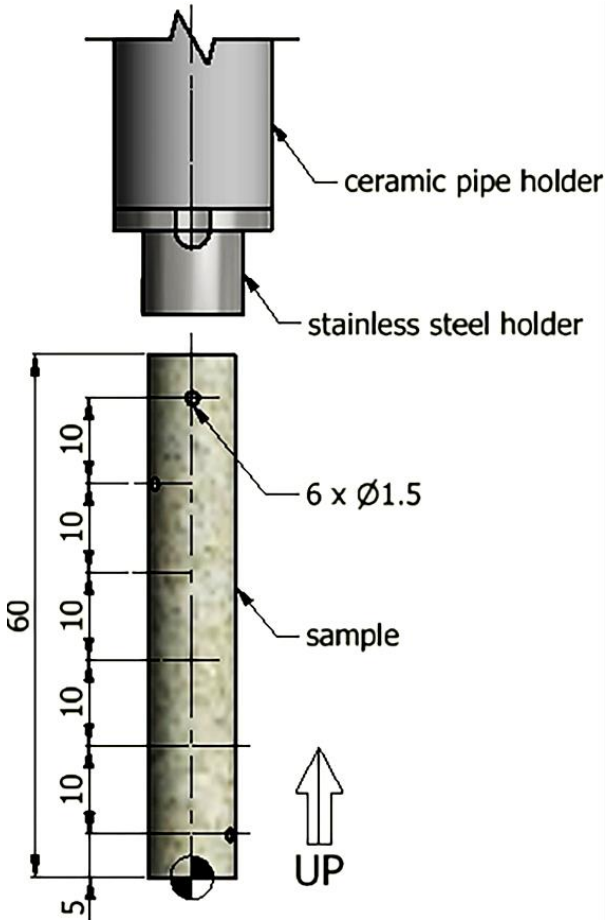

Fig. 2. Clay mold and thermocouples position details.

2.2 Methods

The scheme of equipment is referred to [18] and presented in Fig. 3.

The sample was set in the Bridgman apparatus; it was heated up to 650°C at a 1.9 °C/s heat rate and kept for 5 minutes [19]. Next, the sample was withdrawn at 0.04 mm/s, and the cooling system was activated simultaneously. The furnace was still active during cooling to ensure the heat transfer was only in the vertical direction. A data logger, PLX-DAQ, and Arduino Uno system recorded the temperature throughout the cooling, and it was stopped if the temperature at 55 mm was lower than the solidus temperature.

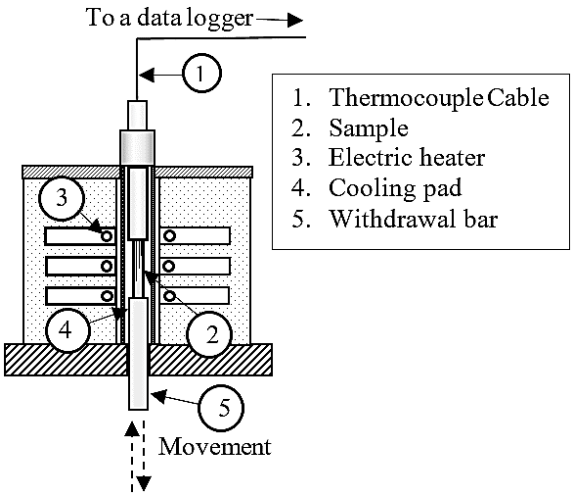

Fig. 3. Scheme of equipment.

The cooling curves were generated from the recording temperatures at 5, 15, 25, 35, 45, and 55 mm from the contact area. A representation of the cooling curve for samples was plotted to observe the influence of the grain refiner. The representation curve is made from the recorded temperature data at 15 mm. Prior to the calculation of the solidification parameters, the liquidus and solidus temperatures at the selected composition were determined based on the Al-Cu-Si at 10wt.%Si phase diagram by Pan [20]. These temperatures (560.85 and 521.91°C) were the boundaries of the freezing zone of Al-10wt.%Cu-10wt.%Si. The cooling rate, growth rate, temperature gradient, and local solidification time were calculated within this zone. The calculation method was referred to in [21], [22], [23], and [24].

The preparation and metallography test procedures were applied to both sample types. The first step was sectioning the samples across their length, and then metallography sample preparation procedures were applied without etching. Microstructure observations were conducted using a metallurgical microscope (Olympus, Japan). The observations were made at 1, 5, 10, 20, 25, 35, 40, and 45 mm from the contact area.

3 Results and Discussion

A representation of the cooling curve of both samples is shown in Fig. 4.

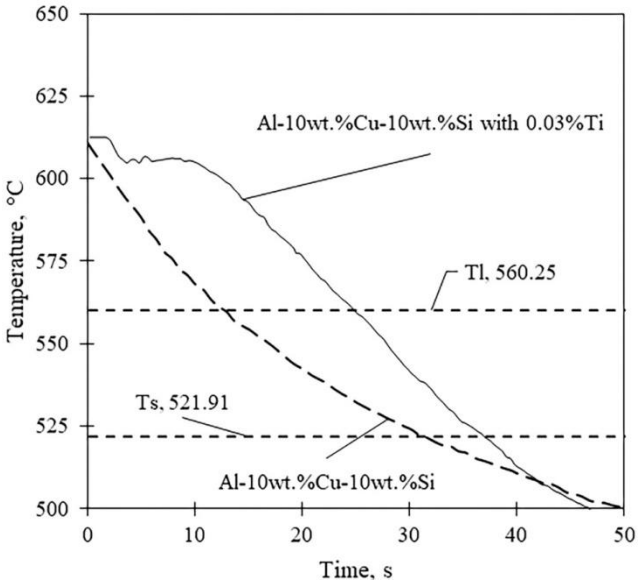

Fig. 4. Cooling curve of Al-10wt.%Cu-10wt.%Si with and without 0.03wt.%Ti.

The cooling curve of 0.03wt.%Ti in the freezing is mainly about 39.25 to 16.5°C above the base alloy zone. The cooling slope of 0.03wt.%Ti is higher than the cooling slope of the base

alloy. This condition indicates the solidification process of 0.03wt.%Ti is faster than that of the base alloys. The base alloy starts to solidify at 13 s and ends at 31 s, while the solidification of 0.03wt.%Ti begins at 25 s and finishes at 36.8 s. The process is 6 s faster than the base alloys. The addition of 0.03wt.%Ti increases the temperature and slope of the cooling curve, yet it shortens the solidification time.

The solidification parameters of 0.03wt.%Ti and the base alloy are presented in Fig. 5. Generally, they decline with the distance, except for the local solidification time.

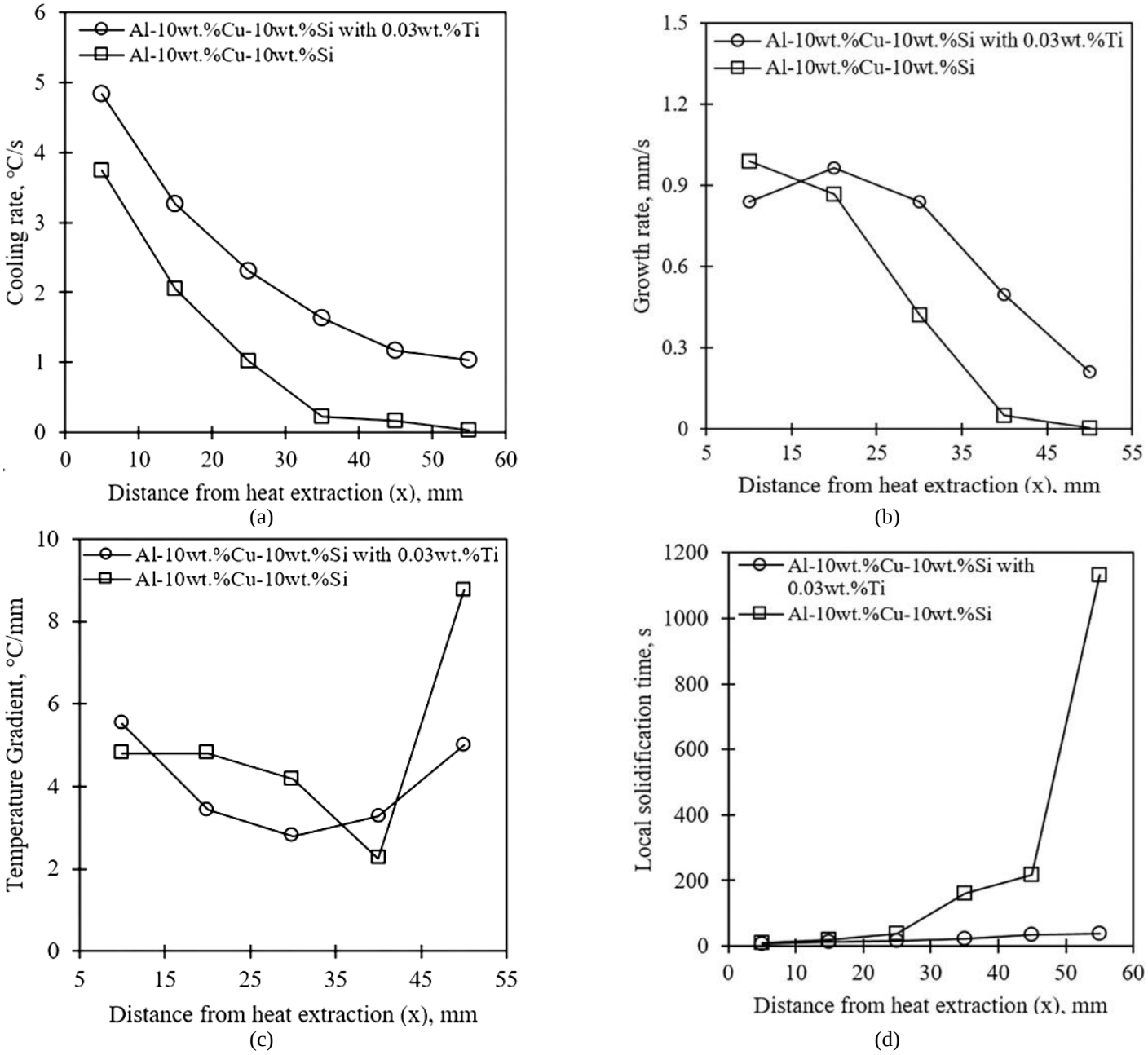

Fig. 5. Solidification parameters (a. Cooling rate, b. Growth rate, c. Temperature gradient, d. Local solidification time) across sample length.

The cooling and growth rate of 0.03wt.%Ti are 1-1.1 °C/s and 0.09-0.45 mm/s over the base alloy, respectively (Fig. 5(a) and Fig. 5(b)). The temperature gradient of 0.03wt.%Ti decreases from 5.5 °C/mm at 10 mm to 2.8 before rising to 5 °C/mm at 50 mm (Fig. 5(c)). The base alloy's temperature gradient declines from 4.8 °C/mm at 10 mm to 2.3 °C/mm at 40 mm, then rises to 8.75 °C/mm at 50 mm. The local solidification time shows a vice versa of the cooling rate data (Fig. 5(d)). The local solidification time of the base alloy is 2.05 to 1093.64 s above the 0.03wt.%Ti.

The micrograph images across the length of 0.03wt.%Ti are presented in Fig. 6. Fine columnar dendrite structures are seen at 1 mm; some grow parallel to the solidification direction (a), and others grow at random (b). The fine columnar structures (a) is seen at 5 mm; above this structure, a fine equiaxed structure is formed (c). No more columnar is found in 10 mm; two structures are available: fine equiaxed (c) and large equiaxed (d). The large equiaxed with growing branches in the dendrite form is spotted at 20 and 25 mm (e-f). The branches are dominantly in the vertical direction, but with the increasing distance to 35-45 mm, more horizontal branches (i) and large sizes of equiaxed dendrites are found (g). The microstructure of 0.03wt.%Ti undergoes non-uniform structures: fine columnar, fine equiaxed, coarse equiaxed, and dendrite equiaxed.

Fig. 7 presents the micro-structures of the base alloy across the sample length. The nucleation sites were only seen at 1 mm; the nuclei grow in narrow spacing and form fine columnar structures (a). Fine columnar is seen at 1 to 10 mm, the second branch thicken (b) at 10 to 25 mm, and the space between the dendrite increases. The third branch start to grow (c) at 25 mm, and finally, the coarse columnar structures (d) are found at 35 to 45 mm. Long columnar structures are seen at all observed distances. Many nucleation sites are unlikely to occur in the Al-10wt.%Cu-10wt.%Si sample.

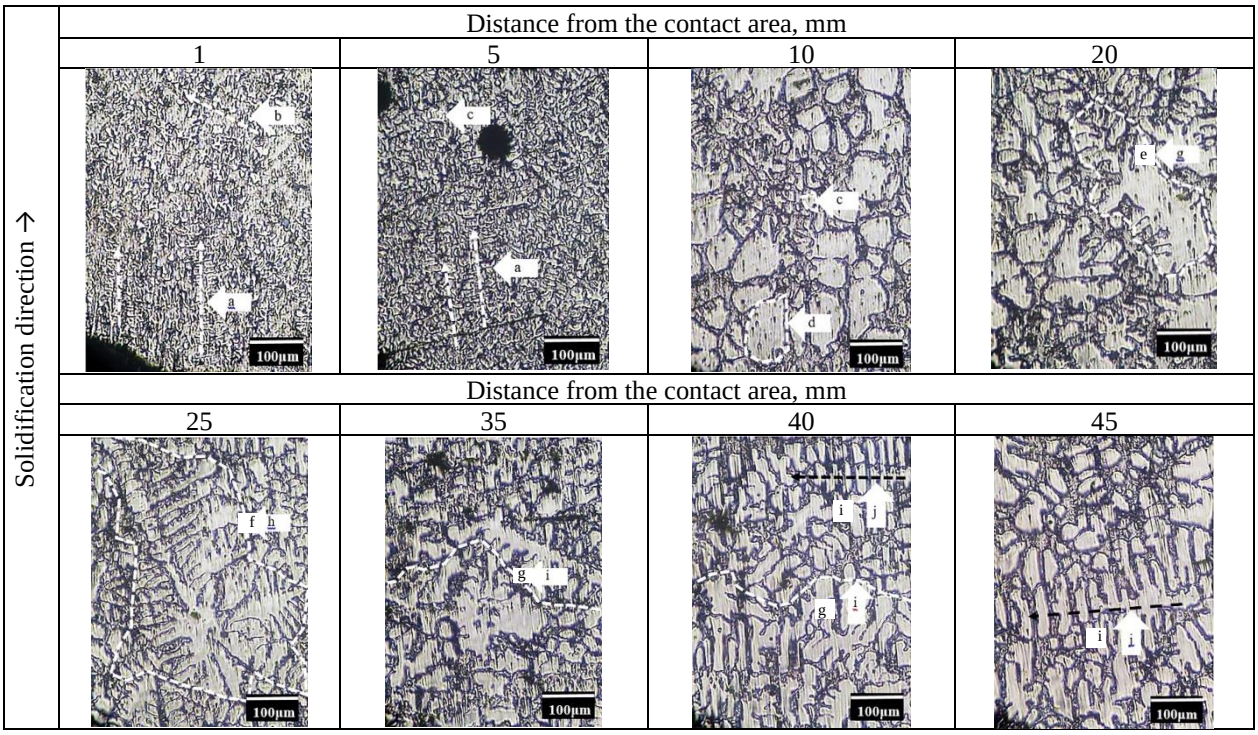

Fig. 6. Microstructures of Al-10wt.%Cu-10wt.%Si with 0.03wt.%Ti across the sample length.

The cooling curve indicates an uplift of the temperature on 0.03wt.%Ti about 39.25 to 16.5°C above the cooling curve of the base alloy in the freezing zone. The uplift in temperature is also reported in [7], [12], [16], and [25]. Al-Ti-B was separated into titanium aluminide ($TiAl_3$) and titanium diboride (TiB_2) when it was added to the melt [12]. Millions of $TiAl_3$ crystals were released into the melt and formed nucleates. The $TiAl_3$ was responsible for the rising nucleation temperature above the liquidus point by forming high-energy planes as duplex particles with boride particles [26]. Moreover, it reduced the recalescence by increasing the undercooling temperature [11], promoted an early synthesis, and increased the number of nucleation primers [7]. The evidence is seen in the fine columnar structures on 0.03wt.%Ti sample at 1 to 5 mm (Fig. 6). Two reasons attribute to the formation of fine columnar structures in this area: first, the massive heat transfer that provides a high cooling rate (Fig. 5(a)) and less solidification time (Fig. 5(d)); second, the presence of $TiAl_3$ and TiB_2. This result agrees with [16]; TiB_2 addition refines the columnar structures by accelerating the nucleation crystal in the contact area.

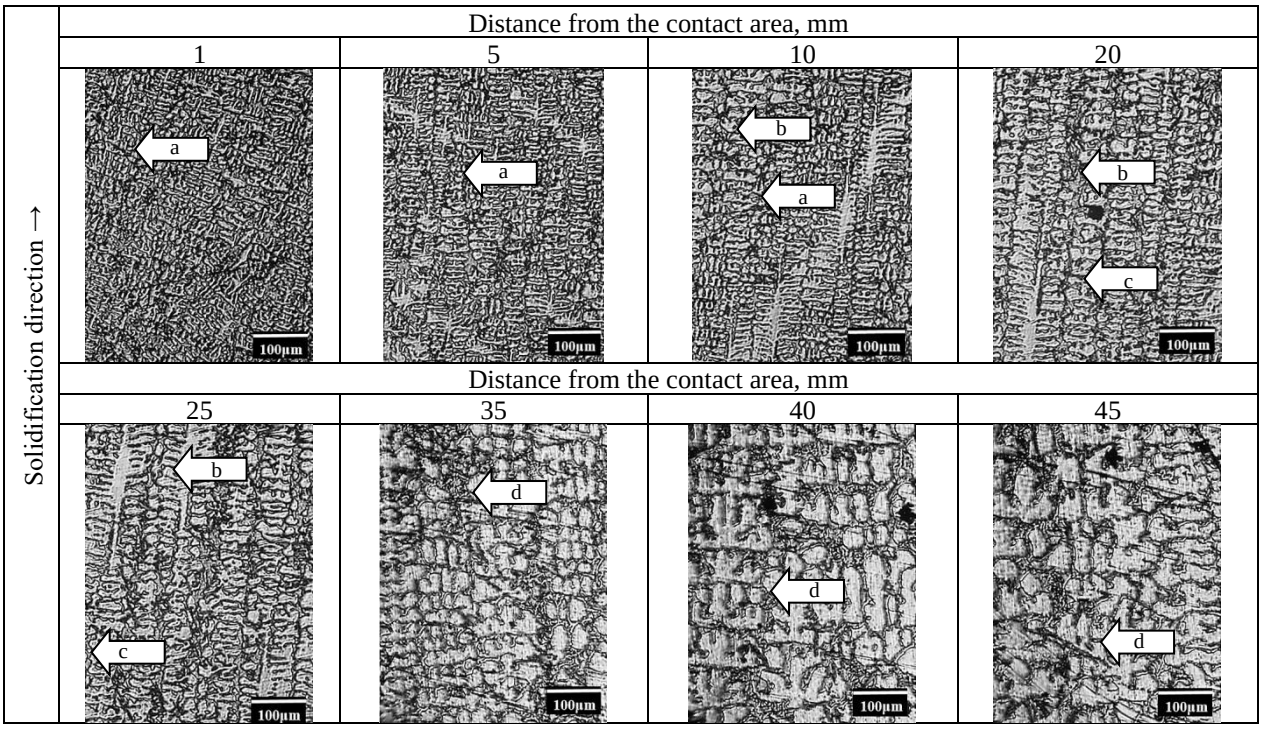

Fig. 7. Microstructures of Al-10wt.%Cu-10wt.%Si without 0.03wt.%Ti across the sample length.

The nucleation temperature is higher than the growth temperature; therefore, α-crystal formed not only in the contact area but also in the melt [7]. This condition prevented the growth of the columnar structures in the contact area. Fig. 8 shows the formation of equiaxed structures that blocked the columnar structures.

As the distance increases, the heat transfer becomes less effective, providing enough time for the structure to grow. The equiaxed morphology increases size, altering their morphologies to dendrite form (Fig. 6 at 20 to 45 mm). A minimum cooling rate is needed to achieve successful grain refinement, and different cooling conditions lead to various degrees of refinement [17]. This

mechanism is in line with [7], [11], [12], and [13], where the aluminum crystal grows around the surface of the $TiAl_3$ crystal. For extended cooling, dendritic growth begins until the solidification process ends.

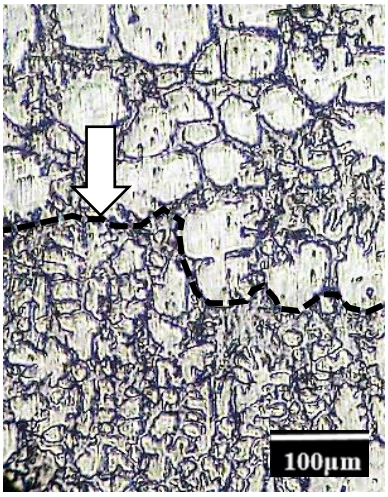

Fig. 8. The equiaxed structures block the columnar structure between 5 to 10 mm from the contact area.

This work has demonstrated that the addition of Al-Ti-B promotes many nucleation sites. These sites prevent the growth of columnar structures in unidirectional solidification. Moreover, the grain refining mechanism is applied at a cooling rate of less than 3.27 °C/s and an addition of 0.03wt.%Ti effectively controls the microstructure in this area. In contrast to the direct casting within this Ti composition, the mechanism is applied in all areas [27]. Further investigation at higher Ti is required to understand whether it can be effectively used to control the microstructure in directional solidification.

In contrast to the mechanism in 0.03wt.%Ti, the columnar structure grows in a very well manner. The sample was composed of a typical columnar structure. Columnar structures are seen at every observation point, and they are coarsening as the distance increases. The size of the microstructure is increasing toward the high temperature [28]. Their morphology alters mostly due to the changing in heat transfer and cooling slope [29], which reflects the variation in solidification parameters variation (Fig. 5). The contact area imposes a higher cooling rate, and as the distance from the contact increases, the cooling rate decreases due to the increase in thermal resistance of solidified shells [30]. These influences translate to the primary and secondary arm spacing values; these values decrease as the cooling rate increases [31]. The evidence is seen in the formation of the fine columnar structures at 1 and 5 mm, and as the cooling rate decreases, the coarse structure with more inter-dendritic space is found at 25 to 55 mm. The coarsening mechanism is attributed to the decline of the cooling rate and the increase in dendritic arm spacing. This condition is also observed in [5], [21], and [32].

4 Conclusion

The Al-Ti-B addition in directionally solidified Al-10wt.%Cu-10wt.%Si uplifts the cooling curve temperature around 39.25 to 16.5°C, increasing the cooling and growth rate. Due to Ti's presence, the decreasing cooling rate, growth rate, and temperature gradient with distance impose a typical implication on the microstructure. Four types of microstructures-fine columnar, fine equiaxed, coarse equiaxed, and equiaxed dendrite-exist, while columnar structures are present in the base alloys. The grain refinement mechanism with 0.03wt.%Ti is dissimilar within the direct casting process, especially at a 4.8 °C/s cooling rate. The Al-Ti-B addition is not recommended in the manufacturing industry, as it requires forming columnar structures in their components.

Acknowledgements

The authors are thankful to the Ministry of Research, Technology and Higher Education of the Republic of Indonesia, and Indonesia Endowment Fund for Education (LPDP) for financial support with contract no. PRJ-1435/LPDP.4.

References

[1] N. K. Dien, T. T. Tho, N. V. Thanh, N. V. A. Duy, A. Jannifar, and N. H. Tho, "Application of topology optimization technique in sand casting process of a complex product based on FDM 3D printing technology," vol. 19, 2021.

[2] A. Akhyar, "Numerical-hydrodynamic analysis, vickers hardness, and tensile test of cast-brass alloy for boat propellers," *Jurnal Polimesin*, vol. 21, no. 2, Apr. 2023, doi: 10.30811/jpl.v21i2.3743.

[3] J. G. Kaufman and E. L. Roy, *Aluminum Alloy Castings: Properties , Processes , and Applications.* 2004.

[4] S. Khan, A. Ourdjini, Q. S. Named, M. A. Alam Najafabadi, and R. Elliott, "Hardness and mechanical property relationships in directionally solidified aluminium-silicon eutectic alloys with different silicon morphologies," *Journal of Materials Science*, vol. 28, no. 21, pp. 5957–5962, 1993, doi: 10.1007/BF00365208.

[5] D. Masnur, Suyitno, and V. Malau, "The Influence of Mold Material on Cooling Curve, Solidification Parameters, and Micro-hardness of Al–6wt .% Si in Unidirectional Solidification," *IOP Conf. Series: Materials Science and Engineering*, vol. 547, 2019, doi: 10.1088/1757-899X/547/1/012014.

[6] M. Farkašová, E. Tillová, and M. Chalupová, "Modification of Al-Si-Cu cast alloy," *FME Transactions*, vol. 41, no. 3, pp. 210–215, 2013.

[7] G. Timelli, G. Camicia, and S. Ferraro, "Effect of grain refinement and cooling rate on the microstructure and mechanical properties of secondary Al-Si-Cu alloys," *Journal of Materials Engineering and Performance*, vol. 23, no. 2, pp. 611–621, 2014, doi: 10.1007/s11665-013-0757-y.

[8] L. Bolzoni, M. Xia, and N. H. Babu, "Formation of equiaxed crystal structures in directionally solidified Al-Si alloys using Nb-based heterogeneous nuclei," *Nature Publishing Group*, no. December, pp. 1–10, 2016, doi: 10.1038/srep39554.

[9] M. Nowak, L. Bolzoni, and N. Hari Babu, "Grain refinement of Al-Si alloys by Nb-B inoculation. Part I: Concept development and effect on binary alloys," *Materials and Design*, vol. 66, no. PA, pp. 366–375, 2015, doi: 10.1016/j.matdes.2014.08.066.

[10] M. Okayasu, S. Takeuchi, S. Wu, and T. Ochi, "Effects of Sb, Sr, and Bi on the material properties of cast Al-Si-Cu alloys produced through heated mold continuous casting," *Journal of Mechanical Science and Technology*, vol. 30, no. 3, pp. 1139–1147, 2016, doi: 10.1007/s12206-016-0218-2.

[11] Q. Wang, Y. X. Li, and X. C. Li, "Grain Refinement of Al – 7Si Alloys and the Efficiency Assessment by Recognition of Cooling Curves," *Metallurgical and Materials Tranactions A*, vol. 34, no. May, pp. 1175–1182, 2003.

[12] G. K. Sigworth and T. A. Kuhn, "Grain refinement of aluminum casting alloys," *International Journal of Metalcasting*, vol. 1, no. 1, pp. 31–40, 2007, doi: 10.1361/asmhba0005302.

[13] Z. Fan *et al.*, "Grain refining mechanism in the Al / Al – Ti – B system," *ACTA MATERIALIA*, vol. 84, pp. 292–304, 2015, doi: 10.1016/j.actamat.2014.10.055.

[14] K. Kashyap and T. Chandrashekar, "Effects and mechanisms of grain refinement in aluminium alloys," *Bulletin of Materials Science*, vol. 24, no. 4, pp. 345–353, 2001, doi: 10.1007/BF02708630.

[15] M. Easton and D. StJohn, “Grain Refinement of Aluminum Alloys : Part I . The Nucleant and Solute Paradigms — A Review of the Literature,” *Metallurgical and Materials Transactions A*, vol. 30, no. June, pp. 1613–1623, 1999, doi: 10.1007/s11661-999-0098-5.
[16] M. Easton and D. StJohn, “Grain refinement of aluminum alloys: Part II. Confirmation of, and a mechanism for, the solute paradigm,” *Metallurgical and Materials Transactions A*, vol. 30, no. June, pp. 1625–1633, 1999, doi: 10.1007/s11661-999-0099-4.
[17] M. Riestra, E. Ghassemali, T. Bogdanoff, and S. Seifeddine, “Interactive effects of grain refinement, eutectic modification and solidification rate on tensile properties of Al-10Si alloy,” *Materials Science and Engineering A*, vol. 703, no. July, pp. 270–279, 2017, doi: 10.1016/j.msea.2017.07.074.
[18] D. Masnur, V. Malau, and S. Suyitno, “Composition Profile and Microstructure Formation of Unidirectionally Solidified Al–4.5 wt% Cu,” *Inter Metalcast*, vol. 16, no. 1, pp. 349–358, Jan. 2022, doi: 10.1007/s40962-021-00598-4.
[19] D. Masnur, V. Malau, and S. Suyitno, “The dependency of the microhardnes on microstructure and solidification parameters of directionally solidified Al–4.5wt.%Cu in clay mold,” *JMES*, vol. 14, no. 3, pp. 7125–7131, Sep. 2020, doi: 10.15282/jmes.14.3.2020.13.0558.
[20] V. Raghavan, “Al-Cu-Si (aluminum-copper-silicon),” *Journal of Phase Equilibria and Diffusion*, vol. 33, no. 1, pp. 59–61, 2012, doi: 10.1007/s11669-012-9982-6.
[21] D. G. Eskin, Q. Du, D. Ruvalcaba, and L. Katgerman, “Experimental study of structure formation in binary Al-Cu alloys at different cooling rates,” *Materials Science and Engineering A*, vol. 405, no. 1–2, pp. 1–10, 2005, doi: 10.1016/j.msea.2005.05.105.
[22] W. Desrosin, L. Boycho, V. Scheiber, C. M. Méndez, C. E. Schvezov, and A. E. Ares, “Evolution of Metallographic Parameters during Horizontal Unidirectional Solidification of Zn-Sn Alloys,” *Procedia Materials Science*, vol. 8, pp. 968–977, 2015, doi: 10.1016/j.mspro.2015.04.158.
[23] H. Kaya, U. Böyük, E. Çadirli, and N. Maraşli, “Influence of growth rate on microstructure, microhardness, and electrical resistivity of directionally solidified Al-7 wt% Ni hypo-eutectic alloy,” *Metals and Materials International*, vol. 19, no. 1, pp. 39–44, 2013, doi: 10.1007/s12540-013-1007-4.
[24] E. Çadirli, “Effect of solidification parameters on mechanical properties of directionally solidified Al-Rich Al-Cu alloys,” *Metals and Materials International*, vol. 19, no. 3, pp. 411–422, 2013, doi: 10.1007/s12540-013-3006-x.
[25] S. Farahany, Mohd. H. Idris, A. Ourdjini, F. Faris, and H. Ghandvar, “Evaluation of the effect of grain refiners on the solidification characteristics of an Sr-modified ADC12 die-casting alloy by cooling curve thermal analysis,” *J Therm Anal Calorim*, vol. 119, no. 3, pp. 1593–1601, Mar. 2015, doi: 10.1007/s10973-014-4367-1.
[26] M. Johnsson, L. Backerud, and G. K. Sigworth, “Study of the mechanism of grain refinement of aluminum after additions of Ti- and B-containing master alloys,” *Metallurgical Transactions A*, vol. 24, no. 2, pp. 481–491, 1993, doi: 10.1007/BF02657335.
[27] M. Vončina, J. Medved, L. Jerina, I. Paulin, P. Cvahte, and M. Steinacher, “The Impact of AL-TI-B Grain-Refiners from Different Manufacturers on Wrought AL-alloy,” *Archives of Metallurgy and Materials*, pp. 739–746, Mar. 2019, doi: 10.24425/amm.2019.127607.
[28] M. Buchmann and M. Rettenmayr, “Microstructure evolution during melting and resolidification in a temperature gradient,” *Journal of Crystal Growth*, vol. 284, no. 3–4, pp. 544–553, 2005, doi: 10.1016/j.jcrysgro.2005.06.044.
[29] A. Kolahdooz, S. Nourouzi, M. Bakhshi, and S. J. Hosseinipour, “Investigation of the controlled atmosphere of semisolid metal processing of A356 aluminium alloy,” *Journal of Mechanical Science and Technology*, vol. 28, no. 10, pp. 4267–4274, 2014, doi: 10.1007/s12206-014-0940-6.
[30] O. L. Rocha, C. A. Siqueira, and A. Garcia, “Heat flow parameters affecting dendrite spacings during unsteady-state solidification of Sn-Pb and Al-Cu alloys,” *Metallurgical and Materials Transactions A*, vol. 34, no. 4, pp. 995–1006, 2003, doi: 10.1007/s11661-003-0229-3.
[31] M. Gündüz, H. Kaya, E. Çadırlı, N. Maraşlı, K. Keşlioğlu, and B. Saatçi, “Effect of solidification processing parameters on the cellular spacings in the Al–0.1wt% Ti and Al–0.5wt% Ti alloys,” *Journal of Alloys and Compounds*, vol. 439, no. 1–2, pp. 114–127, Jul. 2007, doi: 10.1016/j.jallcom.2006.08.246.
[32] A. J. Vasconcelos, R. H. Kikuchi, A. S. Barros, and T. A. Costa, “Interconnection between microstructure and microhardness of directionally solidified binary Al-6wt .% Cu and multicomponent Al-6wt .% Cu-8wt .% Si alloys,” *Annals of the Brazilian Academy of Sciences*, vol. 88, no. 2, pp. 1099–1111, 2016, doi: 10.1590/0001-3765201620150172.